Available online at www.sciencedirect.com
SCIENCE DIRECT®
Bioorganic & Medicinal Chemistry
ELSEVIER
Bioorganic & Medicinal Chemistry 12 (2004) 1657–1666

Determination of 3^1-stereochemistry in synthetic bacteriochlorophyll-*d* homologues and self-aggregation of their zinc complexes

Hitoshi Tamiaki,* Hiroyuki Kitamoto, Akiyoshi Nishikawa, Takuya Hibino and Reiko Shibata

Department of Bioscience and Biotechnology, Faculty of Science and Engineering, Ritsumeikan University, Kusatsu, Shiga 525-8577, Japan

Received 17 November 2003; accepted 15 January 2004

Abstract—Zinc complex of methyl 3^1-octadecyl-bacteriopheophorbide-*d* was prepared from modification of naturally occurring chlorophyll-*a*. The 3^1-epimerically pure samples were obtained by HPLC separation and their stereochemistry including the absolute configuration at the secondary alcoholic 3^1-position was determined by combination of esterification to methoxy(trifluoromethyl)phenylacetate and NMR spectroscopy (Mosher's method). Both the epimers were monomeric in a polar organic solvent and self-aggregated in a non-polar solvent to give oligomers as well as dimers possessing red-shifted visible absorption bands. Visible spectra of the non-polar organic solutions were dependent upon the 3^1-chirality and such a diastereoselective control on the self-aggregation led to the formation of self-aggregates with different supramolecular structures.

1. Introduction

Most naturally occurring porphyrins and chlorophylls have some chirality in the molecule and the stereochemistry plays an important role in the construction of natural systems. Chiral secondary alcohols are particularly seen in several molecules including hemes-*a*/*o*,[1] 8^1-hydroxychlorophyll-*a*[2] and bacteriochlorophyll(BChl)s-*c*/*d*/*e*[3,4] as shown in Figure 1. The former two types have one of the stereoisomers found as 3^1S- and 8^1R-stereoisomers, respectively. The latter BChls-*c*/*d*/*e* have epimeric mixtures on the 1-hydroxyethyl group at the

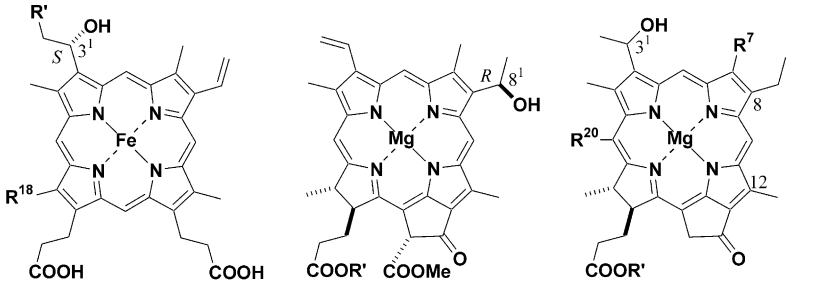

Figure 1. Molecular structures of naturally occurring cyclic tetrapyrrole pigments with a chiral secondary alcoholic moiety (**R′ = farnesyl**).

Keywords: Bacteriochlorophyll; Chlorophyll; Diastereoselectivity; Self-aggregation; Stereochemistry.
* Corresponding author. Tel.: +81-77-566-1111; fax: +81-77-561-2659; e-mail: tamiaki@se.ritsumei.ac.jp

0968-0896/$ - see front matter © 2004 Elsevier Ltd. All rights reserved.
doi:10.1016/j.bmc.2004.01.031

3-position. The $3^1R/S$-stereochemistry has been investigated and determined by several procedures.

Risch and Brockmann first reported the determination of the 3^1-stereochemistry of BChls-*c*/*d*/*e* as follows.[5] An 8,12-homologous mixture of BChl-*c* (or *d*, *e*) from photosynthetic green bacteria was converted to methyl bacteriopheophorbides-*c* (or *d*, *e*) through demetallation and trans-methylation at the 17-propionate. The resulting chiral secondary alcohols were analyzed by Horeau's method based on the stereoselective esterification with (*R*)/(*S*)-2-phenylbutyric acid, suggesting that these BChls-*c*/*d*/*e* should be a 3^1R-rich stereoisomer. Later, Brockmann and Tacke-Karimdadian reported the 3^1-stereochemical determination of the above BChl-*d* with less ambiguity.[6] A homologous mixture of methyl bacteriopheophorbides-*d* was esterified at the 3^1-position with benzoyl chloride and oxidatively cleaved to give *O*-benzoyllactic acid. After methyl-esterification, the resulting lactate was compared with the stereochemically determined authentic sample by optical rotatory, indicating that the *R*-configuration was major at the 3^1-chiral center in the BChl-*d* mixture. Smith et al. unambiguously determined the stereochemistry by crystal structural analysis.[3] Some structurally pure methyl bacteriopheophorbides-*d* gave single crystals suitable for X-ray crystallographic analysis and their 3^1-stereochemistry was clearly confirmed. Based on the analyses, they also assumed the 3^1-configuration of the other BChls by combination of chemical shifts at the *meso*-protons of methyl bacteriopheophorbides with their eluted bands in HPLC. We have already proposed a simple procedure assigned by the elution pattern of 3^1-diastereomeric BChls and their zinc analogues in reverse phase HPLC: a 3^1R-isomer moved faster than the corresponding *S*-isomer in an octadecylated silica column with aqueous methanol as an eluent.[4,7,8]

Now, the stereochemistry of a chiral secondary alcohol has been determined by original and modified Mosher's methods with little ambiguity:[9–11] the determination is based on a combination of stereospecific esterification of a chiral secondary alcohol with (*R*)- or (*S*)-$Ph(CH_3)C(OCH_3)COOH$ and ^1H and ^{19}F NMR spectral analyses of the resulting diastereomeric esters. Here we report synthesis of 3^1-epimerically pure metal-free BChl-*d* homologues possessing a 3^1-octadecyl group instead of the original methyl group, determination of the stereochemistry by Mosher's method and diastereoselective self-aggregation of their zinc complexes in a non-polar organic solvent.

2. Results and discussion

2.1. Determination of the 3^1-stereochemistry in methyl bacteriopheophorbide-*d* (1) by Mosher's method

The absolute configuration at the 3^1-position of methyl bacteriopheophorbide-*d* (**1**, Scheme 1) was determined earlier.[7,12–14] An epimeric mixture of zinc complexes **Zn-1** was readily separated by single HPLC run and the separated epimers were demetallated to give epimerically pure 3^1R-**1R** and 3^1S-**1S**.[7] Compound **1R** was treated with commercially available (*R*)-α-methoxy-α-(trifluoromethyl)phenylacetyl chloride ((*R*)-MTPA-Cl) in dry pyridine to afford the corresponding ester **2R-R** (see Scheme 1). Similarly, reaction of **1R** with (*S*)-MTPA-Cl gave **2R-S** as a Mosher's ester. ^{19}F NMR spectra of **2R-R** and **2R-S** were measured in $CDCl_3$ to give chemical shifts (δ_Fs) of −72.19 and −72.97 ppm, respectively. The δ_F of **2R-S** was higher-field shifted than that of **2R-R**: the difference $\Delta\delta_F$(**2R**) [$=\delta_F$(**2R-S**) — δ_F(**2R-R**) $=-0.78$ ppm] was negative (see Fig. 2A). This shift is consistent with Mosher's prediction for determination of the stereochemistry of chiral secondary alcohol **1R**.[9] The result shows that this method is useful for determination of 3^1-stereochemistry of bacteriopheophorbides.

Recently, modified Mosher's method was reported[10] where ^1H NMR spectra of both the MTPA esters of an epimerically pure secondary alcohol were used. Proton chemical shifts (δ_Hs) of 3^1-methyl group in **2R-R** and **2R-S** were measured in $CDCl_3$ to be 2.26 and 2.34 ppm, respectively. The difference $\Delta\delta_H$(**2R**) [$=\delta_H$(**2R-S**) — δ_H(**2R-R**) $=+0.08$ ppm] in the 3^1-CH_3 was positive (see Fig. 2A). In contrast, most of the $\Delta\delta_H$ at the assigned protons on the peripheral positions of chlorin π-system gave negative or zero values except for the 8^1-/18-CH_3 groups. The negative values gradually increased with increase in the distance from the 3^1-chiral position and

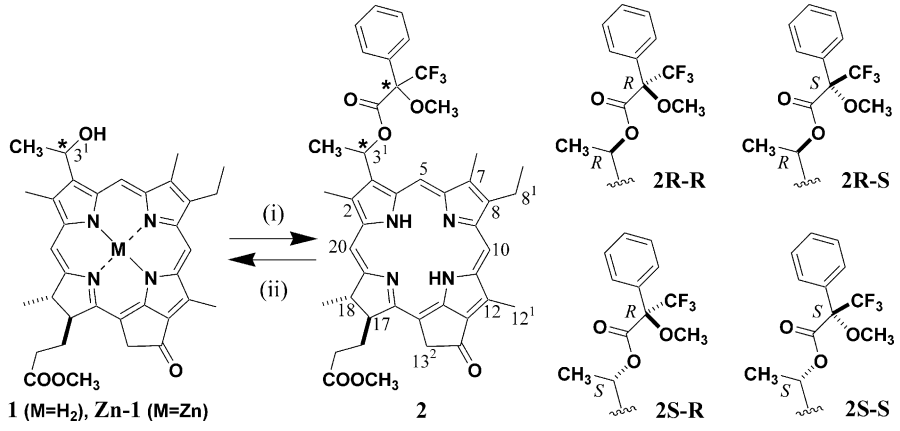

Scheme 1. Synthesis of MTPA ester **2** of methyl bacteriopheophorbide-*d* (**1**); (i) MTPA-Cl/dry C_5H_5N; (ii) K_2CO_3/MeOH.

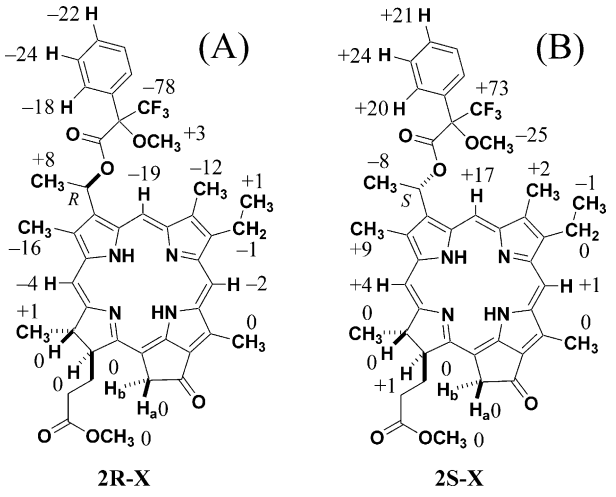

Figure 2. 100-Fold differences ($\Delta\delta'$) between chemical shifts (δ/ppm) of diastereomeric MTPA esters **2** of methyl bacteriopheophorbide-*d*; (A) $\Delta\delta' = [\delta(\mathbf{2R\text{-}S}) - \delta(\mathbf{2R\text{-}R})] \times 100$ and (B) $\Delta\delta' = [\delta(\mathbf{2S\text{-}S}) - \delta(\mathbf{2S\text{-}R})] \times 100$.

reached zero at the 12^1–18 positions. According to the modified Mosher's rule, the secondary alcohol was predicted to have *R*-configuration; this proposed configuration was consistent with the stereochemistry already determined (vide supra). It was recently reported that $\Delta\delta_H$ in the methoxy group of MTPA ester of 1-arylalkanol was useful for determination of stereochemistry of the secondary alcohol: δ_H(heterochiral) — δ_H(homochiral) > 0.[11] In the present case, the $\Delta\delta_H$(**2R**) [$= \delta_H$(heterochiral **2R-S**) — δ_H(homochiral **2R-R**) $= +0.03$ ppm] in the OCH_3 was positive (see Fig. 2A). As a result, another modified Mosher's rule indicated the epimer **1** to be *R*-configuration at the 3^1-position, which was also consistent with the known stereochemistry. Both modified Mosher's methods predicted by ^{1}H NMR spectra are thus applicable for the 3^1-stereochemical determination of bacteriopheophorbides.

The other epimer **1S** was esterified with (*R*)- or (*S*)-MTPA-Cl to give the corresponding ester **2S-R** or **2S-S**, respectively. The original Mosher's method using $\Delta\delta_F$(**2S**) as well as the modified methods using $\Delta\delta_H$(**2S**) showed that the epimer was *S*-configuration at the 3^1-position (see Fig. 2B). MTPA esters of bacteriopheophorbides possessing 1-hydroxyethyl group at the 3-position were available for the absolute configuration of the chiral secondary alcohols. It is noteworthy that the resulting MTPA esters **2** were cleaved with methanol in the presence of potassium carbonate to give the original secondary alcohols **1** [see step (ii) in Scheme 1], and then the present esterification was applied to scanty and valuable samples of naturally occurring pigments because the samples were recovered after the above stereochemical determination.

2.2. Synthesis of methyl 3^1*R*- and *S*-bacteriopheophorbide-*d* homologsue 4 possessing octadecyl group at the 3^1-position

Methyl pyropheophorbide-*d* (**3**, Scheme 2) prepared from chlorophyll-*a* was treated with octadecyl magnesium bromide in tetrahydrofuran to give an 3^1-epimeric

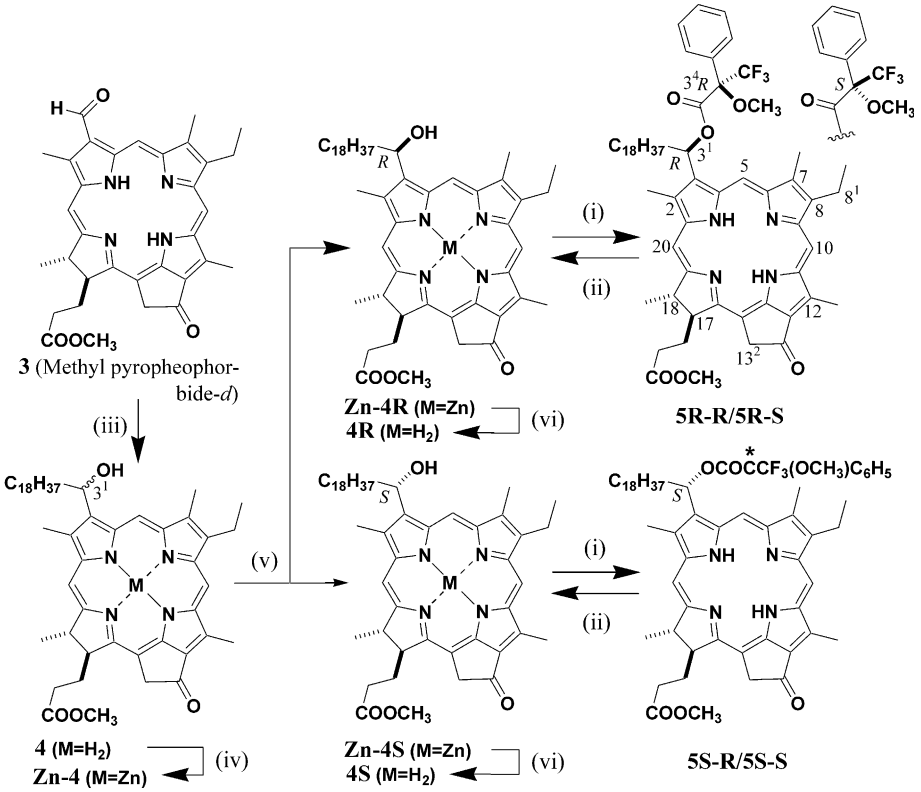

Scheme 2. Synthesis of 3^1-epimerically pure (zinc) methyl 3^1-octadecyl-3^1-demethyl-bacteriopheophorbides-*d* ((**Zn-**)**4R/S**) and their MTPA esters **5**; (i) MTPA-Cl/dry C_5H_5N; (ii) K_2CO_3/MeOH; (iii) $C_{18}H_{37}MgBr$/THF; (iv) $Zn(OAc)_2{\cdot}2H_2O$/MeOH-CH_2Cl_2; (v) HPLC separation; (vi) aq HCl/THF.

mixture of **4** in 44% yield. Such a Grignard reaction is one of the synthetic paths for efficient preparation of various 1-hydroxyalkylated chlorins at the 3- and 8-positions.[15,16] Free base **4** was zinc-metallized and the resulting epimeric mixture **Zn-4** was separated by HPLC to give 3^1*R*-epimer **Zn-4R** and 3^1*S*-epimer **Zn-4S** (see Scheme 2). The separation was slightly more difficult than that of **Zn-1R/S** but was completely achieved by a single run. The separation ratio was 1.8 under the reverse phase HPLC conditions (see Experimental). Separated epimers **Zn-4R/S** were demetallated by action of aqueous diluted acid solution to afford free bases **4R/S**, respectively, without racemization. The access to epimerically pure **4R/S** through zinc-metallation and HPLC-separation followed by demetallation was superior to that by direct separation of **4R/S**, because the latter separation in metal-free compounds was much more difficult even under HPLC conditions than the former in zinc complexes. The epimer prepared from the first HPLC eluting band is called **4#1** and the other from the slow moving band is **4#2**.

3^1-Epimerically pure secondary alcohol **4#1** was esterified with (*R*)- or (*S*)-MTPA-Cl to give the corresponding ester **5#1-R** or **5#1-S**, respectively. $\Delta\delta_F$(**5#1**) = δ_F(**5#1-S**) — δ_F(**5#1-R**) was a negative value of −0.84 ppm (see Fig. 3A). The original Mosher's rule indicates that **4#1** has *R*-configuration at the 3^1-position. Both $\Delta\delta_H$(**5#1**)s of the 3^1-CH_2 group were positive, +0.10 and +0.05 ppm. Most of the $\Delta\delta_H$(**5#1**)s of the protons on the peripheral positions of chlorin π-system were negative or zero except for the 8^1/18-CH_3. $\Delta\delta_H$(**5#1**)s were gradually increased and reached zero in the order: 5-H < 7-CH_3 < 10-H < 12-CH_3 and 2-CH_3 < 20-H < 18-H < 17-H. The modified Mosher's rule shows thus that **4#1** is 4R. $\Delta\delta_H$(**5#1**) of the 3^4-OCH_3 was positive, which is consistent with the other modified Mosher's prediction for **4R**. Therefore, Mosher's rules confirmed that **4#1** has *R*-configuration at the 3^1-position to be **4R**. The fact that 3^1*R*-epimer **Zn-4R** eluted first in a reverse-phase HPLC is consistent with the reported elution rule that the 3^1*R*-epimer of (Zn-)BChl-*c*/*d*/*e*(/*f*) homologues generally eluted faster than the corresponding *S*-epimer under similar HPLC conditions.[4,7,8]

(*R*)- and (*S*)-MTPA esters **5#2-R/S** prepared from **4#2** were analyzed by their ^{1}H and ^{19}F NMR. Both $\Delta\delta_F$(**5#2**) and $\Delta\delta_H$(**5#2**)s as shown in Figure 3B clearly indicated that **4#2** has *S*-configuration at the 3^1-position based on the original and modified Mosher's rules. The absolute configuration at the 3^1-position of epimerically pure **4** obtained from HPLC separation was thus determined. Mosher's methods are useful for stereochemical determination of unnatural 3-(1-hydroxyalkyl)chlorins as in **4** as well as natural 3-(1-hydroxyethyl) analogues as in **1**, and will be applied to other naturally relating pigments including BChls-*c*/*d*/*e*/*f*, hematoporphyrin IX and hemes-*a*/*o*.

2.3. Visible spectral analysis in self-aggregates of methyl 3^1*R*- and *S*-bacteriopheophorbide-*d* homologues 4 possessing octadecyl group at the 3^1-position

3^1*R*/*S*-Epimerically pure **Zn-4R/S** was dissolved in dichloromethane at 3×10^{-5} M to give the same visible spectra (see dotted line of Fig. 4A). The spectra gave sharp Q_y and Soret peaks at 648 and 422 nm, respectively, showing both **Zn-4R/S** to be monomeric in the solution. In 1%(v/v) dichloromethane and hexane, **Zn-4R** (3×10^{-5} M) afforded broadened and red-shifted bands (see solid line of Fig. 4A), compared with the monomeric bands. Typically, 681-nm Q_y band with 690 cm^{-1} of full width at half maximum (FWHM) is situated at 750 cm^{-1} longer wavelength and is 1.8 times wider than the monomeric 648-nm band with FWHM = 380 cm^{-1}. The peaks appearing in the nonpolar organic solvent are ascribable to self-aggregation

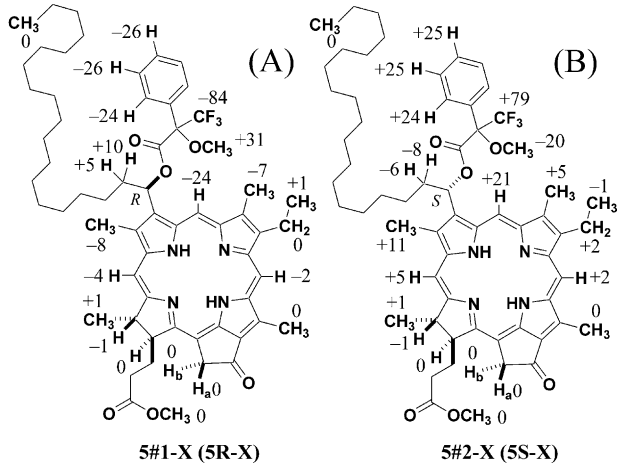

Figure 3. 100-Fold differences (Δδ′) between chemical shifts (δ/ppm) of diastereomeric MTPA esters **5** of methyl 3^1-octadecyl-3^1-demethyl-bacteriopheophorbide-*d*; (A) Δδ′ = [δ(**5#1-S**/**5R-S**)–δ(**5#1-R**/**5R-R**)]×100 and (B) Δδ′ = [δ(**5#2-S**/**5S-S**)–δ(**5#2-R**/**5S-R**)]×100.

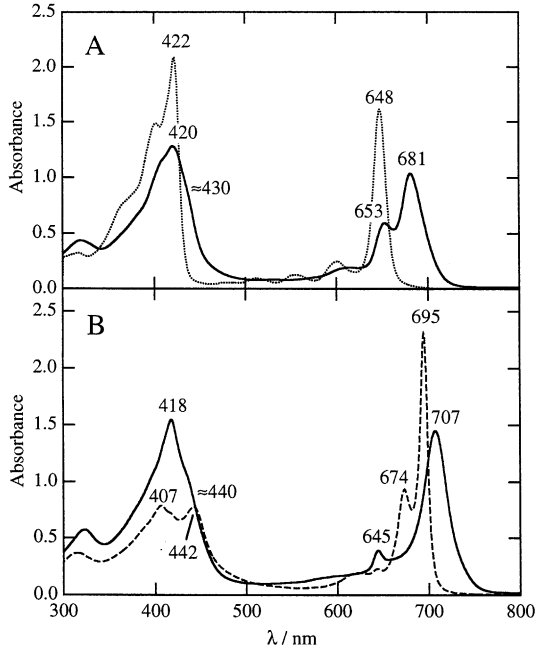

Figure 4. Visible spectra of (A) 3×10^{-5} M **Zn-4R** in CH_2Cl_2 (···) and 1% (v/v) CH_2Cl_2-hexane (—) and (B) 3×10^{-5} M **Zn-4S** in 1%(v/v) CH_2Cl_2–hexane just after preparation of the solution (—) and after standing for 43 h (- - -).

of **Zn-4R**, because of reported similar observation in J-aggregates of **Zn-1**.[7,13,17,18] Under the same conditions, **Zn-4S** showed some different aggregated spectra from that of **Zn-4R**. Just after preparation of the solution, **Zn-4S** gave new major bands at 707 and ca. 440 nm and residual monomeric bands at 645 and 418 nm (see solid line of Fig. 4B). The Q_y peak of self-aggregated **Zn-4S** is more red-shifted than that of **Zn-4R**, while the two FWHMs are almost the same (690/630 cm^{-1} for **Zn-4R/S**). Such a 3^1-diastereomeric control of self-aggregation in **Zn-4R/S** would be due to any difference in the supramolecular structures of self-aggregates of each 3^1-epimer (vide infra). Similar observation has been observed in **Zn-1R/S**[7,13,17,18] as well as in natural BChls-*c*/*d*/*e*.[8,19]

When the non-polar organic solution was allowed to stand at room temperature, the visible spectrum of **Zn-4R** did not change over a week, but that of **Zn-4S** changed greatly on the second day after preparation of the solution. On the first day, no change of the spectrum of **Zn-4S** in the non-polar solution was observed but the spectrum changed drastically during the additional half day to give new species possessing two Q_y peaks at 695 and 674 nm as shown by the broken line of Figure 4B.[20] The resulting species were so stable that no further changes to the original or any other spectra were found for at least a couple of weeks. In the spectrum, small 645 and 418-nm peaks were appeared, indicating that most of the residual monomeric **Zn-4S** decreased during while standing in the solution. Almost all the molecules of **Zn-4S** in the solution finally became the new species. It was first thought that the two Q_y peaks as well as the two Soret peaks (442 and 407 nm) might show the presence of the two species in the solution, but this was ruled out by the following. The new species was gradually deaggregated by addition of pyridine to give a monomeric **Zn-4S** molecule five-coordinated with pyridine as an axial ligand to the central zinc possessing sharp absorption bands at 647 and 423 nm (see Fig. 5). All the self-aggregated spectral bands in Figure 5 were the same shape and the two Q_y peaks decreased at the same ratio. The new and conservative spectrum is thus due to a single species possessing two Q_y and Soret peaks. The above observations were ascribable to the fact that a kinetically controlled and meta-stable self-aggregate of **Zn-4S** as well as the monomer changed to a thermodynamically controlled and relatively stable aggregative species in 1%(v/v) dichloromethane and hexane at room temperature. Such a time dependent spectral change was found in the self-aggregate of **Zn-4S**, not in that of **Zn-4R**. It is worthy of note that another diastereoselective control on the self-aggregation in **Zn-4R/S** operated in the formation rate of their stable self-aggregates.

Monomeric zinc complexes **Zn-4R/S** in dichloromethane changed by dilution of hexane to self-aggregates possessing red-shifted absorption bands and the resulting self-aggregates in the non-polar organic solvent changed by addition of pyridine to the monomer reversibly (vide supra). The sensitivity for deaggregation was dependent on the self-aggregative species. The peak intensity at 681 nm in 1% (v/v) dichloromethane and hexane solution (3 mL) of **Zn-4R** (90 nmol) was halved by about 4 equivalent pyridine (370 nmol). Under the same conditions, the 707-nm peak observed in the freshly prepared self-aggregate of **Zn-4S** reduced to half the intensity by addition of only ca. 0.1 equivalent pyridine (8 nmol). The self-aggregate of **Zn-4S** with two 695 and 674-nm Q_y peaks prepared after standing for two days was deaggregated by pyridine as described above and the stable species resisted the deaggregation as expected. The amount of pyridine for halving these Q_y peak intensities was 2000 times larger (18 μmol, 200 equiv) than that just after preparation. Structural stability of self-aggregates thus increased in the order: self-aggregate of **Zn-4S** (λ_{max} = 707 nm) < self-aggregate of **Zn-4R** (681 nm) < self-aggregate of **Zn-4S** (695/674 nm).

2.4. Proposed supramolecular structures of self-aggregative species (Zn-4R/S)$_n$

Compared with self-aggregates of **Zn-1R** possessing a 3^1-methyl group, **Zn-4R** possessing a longer 3^1-octadecyl group yielded a less red-shifted Q_y peak (681 nm)

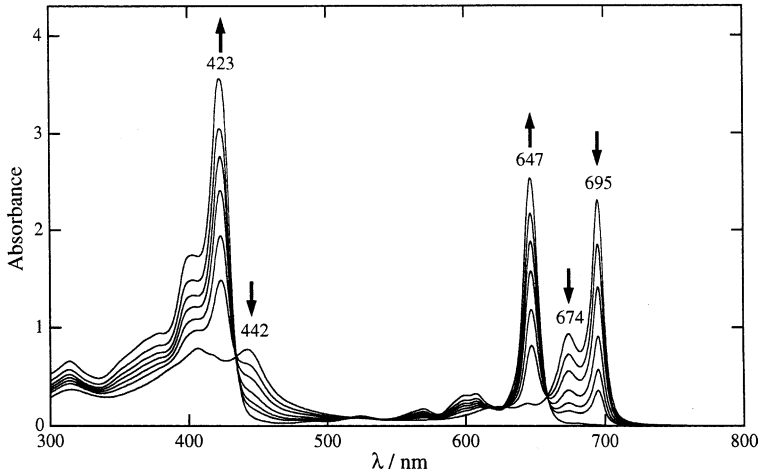

Figure 5. Visible spectral change of **Zn-4S** (90 nmol) in 1% (v/v) CH_2Cl_2–hexane (3 mL, after 2-day standing) by addition of pyridine, 9, 16, 21, 26, 41, 78 μmol.

Table 1. Q_y absorption bands of 3^1-epimeric zinc chlorins **Zn-4R/S** and **Zn-1R/S** in 1%(v/v) CH_2Cl_2-hexane: absorption maximum λ_{max} (nm), full width at half maximum FWHM (cm^{-1}) and red-shift Δ (cm^{-1}) of λ_{max} by self-aggregation [$= \{1/645\,(\text{monomer}) - 1/\lambda_{max}\,(\text{aggregates})\} \times 10^7$]

		λ_{max} [FWHM]	Δ	
Zn-4R		681 [690]	820	this work
		*650[a] [≈500]	120	
Zn-4S	(just after preparation)	707 [630]	1360	this work
		645 [≈300] (monomer)		
	(after standing for 2 days)	695	1120	
		674	670	
Zn-1R		705 [660]	1320	ref 18
Zn-1S		697 [950]	—	ref 18
		*708[b]	1380	
		*702[b]	1260	
		*692[b]	1050	
		645 (monomer)		

[a] An estimated peak from spectral deconvolution analysis.
[b] Estimated peaks from second derivative of 697-nm band.

with almost the same bandwidth accompanied by a small 653-nm peak (see Table 1). From deconvolutional analysis of the spectrum, the latter band was ascribable to a 650-nm band with about 500 cm^{-1} of the FWHM. The estimated peak position (650 nm) has a slightly longer wavelength than the observed peak of the monomeric zinc complexes in the non-polar organic solvent (645 nm), and also the estimated FWHM (≈500 cm^{-1}) is larger than the monomeric (≈300 cm^{-1}). Therefore, the accompanying band is not assigned to a monomeric species but to a small self-aggregate including dimer. The 705-nm band in self-aggregates of **Zn-1R** was reported to come from a large self-aggregate **IV** prepared by a special bond of 13-C=O···H–O···Zn and π-π interaction (see Scheme 3).[17,18] The major 681-nm band in self-aggregates of Zn-4R is assumed to be a fragment of such a large self-aggregate because of the structural similarity between **Zn-1/4R**. Molecular modeling[18] supported that longer $C_{18}H_{37}$ group at the 3^1-position in **Zn-4R** would disturb the hydrogen bonding of the keto-carbonyl group at the 13-position with zinc-coordinated hydroxy group at the 3^1-position and that **Zn-4R** would self-aggregate exclusively by coordination of 3^1-OH to Zn to give a 'step' linear oligomer **III** as an element of large self-aggregates **IV**. A similar step oligomer **III** possessing a ca. 900-cm^{-1} red-shifted Q_y peak has been speculated in the course of formation of large self-aggregates of **Zn-1** on the basis of several spectroscopic analyses,[17] which also supports 681-nm absorbing species to be a step oligomer **III** of **Zn-4R**.

3^1-Epimerically pure **Zn-4S** self-aggregates to form a meta-stable species absorbing at 707 nm in the initial stage. This species is very similar to the self-aggregate of **Zn-1R** at both points of λ_{max} and FWHM (see Table 1). The peak position of self-aggregate of **Zn-4S** is also similar to that of the estimated longest wavelength absorbing peak in self-aggregates of **Zn-1S** (708 nm). These similarities in spectral features lead to the meta-stable self-aggregate of **Zn-4S** having a similar supramolecular structure to the large self-aggregates **IV** observed in **Zn-1R/S**. The structural motif must be the same in all three self-aggregates but the initial self-aggregate of **Zn-4S** was formed by weaker bondings than those of **Zn-1R/S**. A stable species converted irreversibly from the initial self-aggregate of **Zn-4S** is different from the large self-aggregates described above in the visible spectral features of two sharp Q_y peaks. Large circular dichroism (CD) peaks were observed at the same Q_y-absorbing peak positions (Fig. 6B), indicating that two Q_y-directed components are tightly coupled in the species. Considering that the closed dimer in a BChl-*c* molecule with a piggy-back conformation gave two 480-cm^{-1} separated Q_y peaks at 703 and 680 nm with high and low intensities, respectively,[21] the finally prepared species in **Zn-4S** would be similar to a closed dimer **V** consisting of mutual coordination of 3^1-OH of one molecule with Zn of the other (see Scheme 3). The reversed S-shape CD spectrum showed that Q_y transition dipole moments are situated in an anti-clockwise fashion,[22] also supporting the presence of the

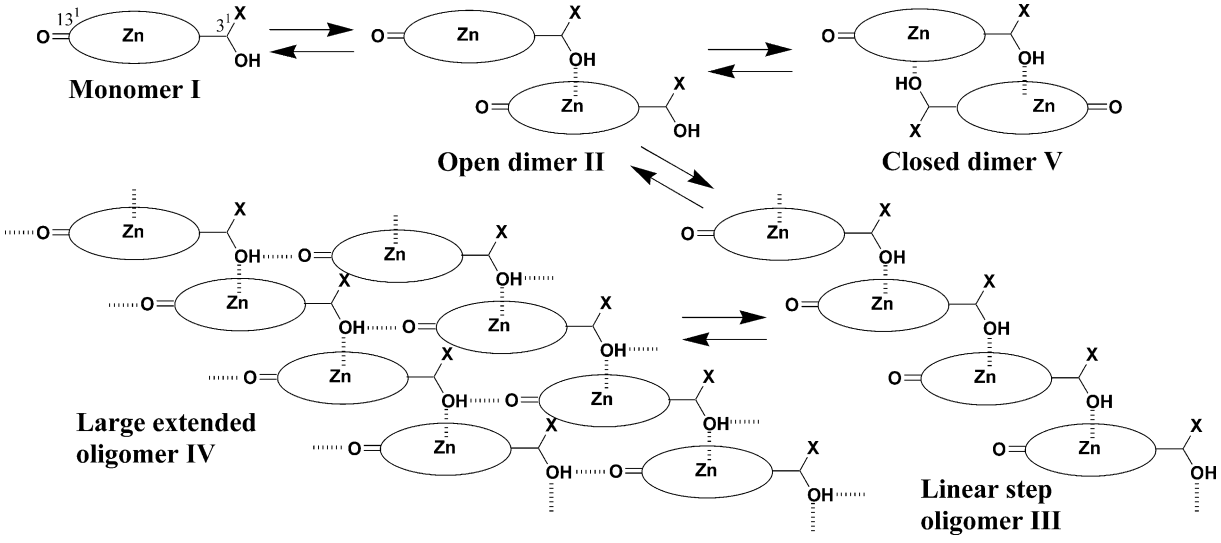

Scheme 3. Schematic drawing of self-aggregation of **Zn-4R/S** ($X = C_{18}H_{37}$) or **Zn-1R/S** ($X = CH_3$).

closed dimeric conformation in the final stage of self-aggregation of **Zn-4S**. Similar closed dimers were reported to be so stable that no more self-assemblies could be observed in the other zinc chlorins.[17,23] It can be generally accepted that such 'dead-end' closed dimers **V** hardly self-aggregate and do not form any other large oligomers. Two zinc-coordinated hydroxy groups in the closed dimer of **Zn-4S** are shielded from any other environments including hexane as a solvent by a sterically large and long octadecyl group at the neighboring position to give the stable dimeric conformation.

2.5. Schemes in self-aggregation of 3^1-epimerically pure zinc complexes Zn-4R/S

3^1*R*-Epimer **Zn-4R** was monomer **I** (see Scheme 3) in diluted dichloromethane solution. In 1%(v/v) dichloromethane and hexane, **Zn-4R** self-aggregated to form a linear step oligomer **III** absorbing 681-nm peak accompanied by a small aggregate possessing a 650-nm band. The small aggregate is tentatively assigned to open dimer **II** (see Scheme 3) because such a dimer is a composition component of the co-existing linear oligomer **III**: the open dimer **II** self-aggregates by coordination of free 3^1-OH of dimer to 4-coordinated and non-axial-ligated zinc of another to form the linear oligomer **III**. The homologous 3^1-methylated **Zn-1R** self-aggregated in the non-polar organic solvent to form large oligomers **IV** through hydrogen bonds of coordinated 3^1-OHs of a linear oligomer **III** to 13-keto carbonyl groups of the other **III**. This difference is ascribable to the steric effect around the 3^1-OH group: the 3^1-OH group in **Zn-4R** is more sterically hindered than that in **Zn-1R**. The special hydrogen bond necessary for preparation of large extended self-aggregates **IV** was hardly formed in **Zn-4R** because of the large octadecyl group near the 3^1-OH.

In contrast, **Zn-4S** self-aggregated in the non-polar organic solvent to form a large self-aggregate **IV** because linear step oligomer **III** of **Zn-4S** is more distorted than that of **Zn-4R** and coordinated 3^1-OHs of a linear oligomeric **Zn-4S** could hydrogen-bond loosely to 13-keto carbonyl groups of the other. The large extended oligomer **IV** of **Zn-4S** just after preparation of the solution is fairly unstable and equilibrates to a small amount of monomer **I**. During standing of the solution at room temperature, the residual monomer **I** dimerized to slowly and irreversibly form quite a stable closed dimer **V**: one day was necessary for the formation under the present conditions. Once the stable dimer **V** was formed, large oligomer **IV** was unstabilized due to a decrease in the number of associated molecules and deaggregated rapidly: a half day was enough for the complete deformation from large oligomer **IV** to closed dimer **V**. The homologous 3^1-methylated **Zn-1S** gave relatively stable large oligomers **IV** because of less steric hindrance around the 3^1-OH and also did not change the closed dimer **V**. This observation is also due to the relative instability of closed dimer **V** of **Zn-1S** because the coordinated 3^1-OH groups in the dimer are exposed to hydrophobic environments.

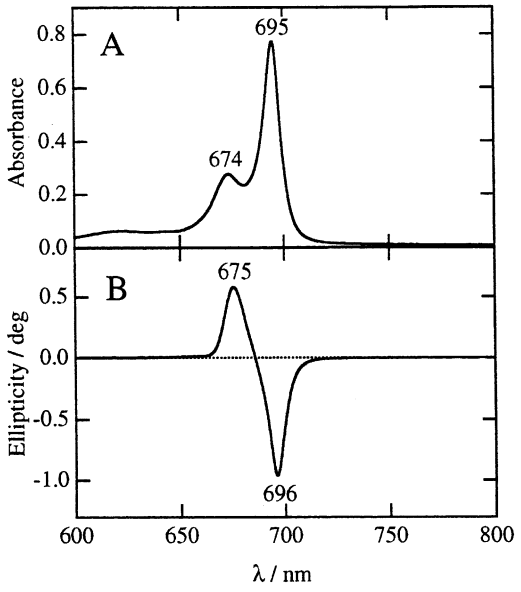

Figure 6. Visible (A) and CD spectra (B) of 1×10^{-5} M **Zn-4S** in 1% (v/v) CH_2Cl_2-hexane after standing for 2 days.

3. Conclusion

Zinc methyl 3^1-epimerically pure 3^1-octadecyl-bacteriopheophorbides-*d* (**Zn-4R/S**) were synthesized from chemical modification of chlorophyll-*a*. The absolute configuration at the 3^1-position was determined by three original and modified Mosher's methods. Visible spectral analyses in 1%(v/v) dichloromethane and hexane solutions showed that 3^1*R*-epimer **Zn-4R** gave mainly 'linear step oligomer **III**' and 3^1*S*-epimer **Zn-4S** gave kinetically controlled and loosely bounded 'large extended oligomer **IV**' followed by the final formation of thermodynamically controlled 'closed dimer **V**'. A long octadecyl group as the 3^1-substituent more greatly affected 3^1-diastereoselective control on the self-aggregation than did either a simple methyl group as in **Zn-1** or natural pigments. The proposed scheme for self-aggregation of zinc 3^1-hydroxy-13^1-oxo-chlorins as in **Zn-1/4** leads to the large extended self-aggregates having supramolecular structures based on 'open dimer **II**' in a parallel stacking fashion and anti-parallel 'closed dimers **IV**' being unable to self-aggregate any more. This scheme would be adapted for natural light-harvesting extramembraneous antenna systems of photosynthetic green bacteria[24] and in vivo self-aggregates of BChls-*c*/*d*/*e* have similar supramolecular structures prepared by stacking in a parallel fashion.

4. Experimental

4.1. Apparatus

Visible absorption spectra were measured with a Hitachi U-3500 spectrophotometer. ^{1}H NMR spectra were measured with a Bruker AC-300 or JEOL JNM-400 spectrometer; chemical shifts (δs) are expressed in parts per million relative to $CHCl_3$ (7.26 ppm) as an internal reference. ^{19}F NMR spectra were measured with a

Bruker AC-300 spectrometer; chemical shifts (δs) are expressed in parts per million relative to CF_3COOH (−77 ppm) as an external reference. Mass spectra were recorded on a JEOL HX-100 or GCmate II spectrometer; FAB-MS samples were dissolved in $CHCl_3$ and *m*-nitrobenzyl alcohol was used as the matrix. HPLC was performed with a Shimadzu LC-10AD*VP* pump, SPD-M10A*VP* diode-array detector and SCL-10A*VP* system controller.

4.2. Materials

3^1-Epimerically pure **1R/S**[7] and **3**[25] were prepared by the reported procedures. All the other chlorin compounds were synthesized by the following procedures in the dark under N_2. THF was distilled from CaH_2 before use. Solvents for visible spectra were purified by distillation over CaH_2.

4.2.1. General procedures of MTPA ester. To a dry pyridine solution (100 μL) of secondary alcohol **1/4** (ca. 3 μmol) was added (*R*)- or (*S*)-MTPA-Cl (10 μL, 53 μmol). After stirring at room temperature for 1 h, the reaction was quenched with *N*,*N*-deimethyl-1,3-propanediamine (15 μL, 120 μmol). The solution was diluted with dichloromethane (20 mL), washed with aqueous 4% sodium hydrogen carbonate and water, dried over sodium sulfate, and evaporated at a reduced pressure. The residue was dissolved in methanol and purified with HPLC (Cosmosil 5C18-ARII 6 or 10 mmϕ×250 mm, H_2O–MeOH, 1.5 mL/min) to give pure MTPA ester **2**/**5**.

4.2.2. 2R-R. 1R and (*R*)-MTPA-Cl gave **2R-R** at retention time (rt) = 36 min (10 mmϕ column, 3% H_2O–MeOH); vis (CH_2Cl_2) λ_{max} = 664 (relative intensity, 0.49), 608 (0.07), 555 (0.03), 536 (0.09), 506 (0.10), 472 (0.04), 410 (1.00), 318 nm (0.20); ^{1}H NMR ($CDCl_3$) δ = 9.57 (1H, s, 10-H), 9.54 (1H, s, 5-H), 8.60 (1H, s, 20-H), 7.54 (1H, q, *J* = 7 Hz, 3-CH), 7.42 (2H, d, *J* = 8 Hz, *o*-H of Ph), 7.13 (1H, t, *J* = 7 Hz, *p*-H of Ph), 6.98 (2H, t, *J* = 8 Hz, *m*-H of Ph), 5.30 (1H, d, *J* = 20 Hz, 13^2-H_a, syn to 17-propionate), 5.14 (1H, d, *J* = 20 Hz, 13^2-H_b, anti to 17-propionate), 4.51 (1H, q, *J* = 7 Hz, 18-H), 4.32 (1H, d, *J* = 8 Hz, 17-H), 3.70 (3H, s, 12-CH_3), 3.70 (2H, *J* = 7.5 Hz, 8-CH_2), 3.63 (3H, s, 17^3-OCH_3), 3.44 (3H, s, 2-CH_3), 3.35 (3H, s, 3^4-OCH_3), 3.12 (3H, s, 7-CH_3), 2.64–2.77, 2.21–2.37 (each 2H, m, 17-CH_2CH_2), 2.26 (3H, d, *J* = 7 Hz, 3^1-CH_3), 1.81 (3H, d, *J* = 7 Hz, 18-CH_3), 1.70 (3H, t, *J* = 7.5 Hz, 8^1-CH_3), 0.27, −1.86 (each 1H, s, NH); ^{19}F NMR ($CDCl_3$) δ = −72.19. MS (FAB) found: *m*/*z* 783. calcd for $C_{44}H_{46}N_4O_6F_3$: MH^+, 783.

4.2.3. 2R-S. 1R and (*S*)-MTPA-Cl gave **2R-S** at rt = 32 min (10 mmϕ column, 3% H_2O–MeOH); vis (CH_2Cl_2) λ_{max} = 664 (rel. 0.53), 608 (0.08), 555 (0.03), 536 (0.10), 506 (0.10), 472 (0.04), 410 (1.00), 318 nm (0.20); ^{1}H NMR ($CDCl_3$) δ = 9.55 (1H, s, 10-H), 9.35 (1H, s, 5-H), 8.56 (1H, s, 20-H), 7.45 (1H, q, *J* = 7 Hz, 3-CH), 7.24 (2H, d, *J* = 8 Hz, *o*-H of Ph), 6.91 (1H, t, *J* = 7 Hz, *p*-H of Ph), 6.74 (2H, t, *J* = 8 Hz, *m*-H of Ph), 5.30 (1H, d, *J* = 20 Hz, 13^2-H_a, syn to 17-propionate), 5.13 (1H, d, *J* = 20 Hz, 13^2-H_b, anti to 17-propionate), 4.50 (1H, q, *J* = 7 Hz, 18-H), 4.32 (1H, d, *J* = 8 Hz, 17-H), 3.70 (3H, s, 12-CH_3), 3.69 (2H, *J* = 7.5 Hz, 8-CH_2), 3.63 (3H, s, 17^3-OCH_3), 3.60 (3H, s, 2-CH_3), 3.38 (3H, s, 3^4-OCH_3), 3.00 (3H, s, 7-CH_3), 2.52–2.76, 2.22–2.37 (each 2H, m, 17-CH_2CH_2), 2.34 (3H, d, *J* = 7 Hz, 3^1-CH_3), 1.82 (3H, d, *J* = 7 Hz, 18-CH_3), 1.71 (3H, t, *J* = 7.5 Hz, 8^1-CH_3), 0.29, −1.88 (each 1H, s, NH); ^{19}F NMR ($CDCl_3$) δ = −72.97. MS (FAB) found: *m*/*z* 782. calcd for $C_{44}H_{45}N_4O_6F_3$: M^+, 782.

4.2.4. 2S-R. 1S and (*R*)-MTPA-Cl gave **2S-R** at rt = 32 min (10 mmϕ column, 3% H_2O–MeOH); vis (CH_2Cl_2) λ_{max} = 664 (rel. 0.50), 607 (0.08), 555 (0.03), 536 (0.09), 505 (0.10), 473 (0.03), 410 (1.00), 319 nm (0.20); ^{1}H NMR ($CDCl_3$) δ = 9.56 (1H, s, 10-H), 9.38 (1H, s, 5-H), 8.56 (1H, s, 20-H), 7.47 (1H, q, *J* = 7 Hz, 3-CH), 7.23 (2H, d, *J* = 8 Hz, *o*-H of Ph), 6.94 (1H, t, *J* = 7 Hz, *p*-H of Ph), 6.78 (2H, t, *J* = 8 Hz, *m*-H of Ph), 5.29 (1H, d, *J* = 20 Hz, 13^2-H_a, syn to 17-propionate), 5.13 (1H, d, *J* = 20 Hz, 13^2-H_b, anti to 17-propionate), 4.51 (1H, q, *J* = 7 Hz, 18-H), 4.32 (1H, d, *J* = 8 Hz, 17-H), 3.70 (2H, q, *J* = 7.5 Hz, 8-CH_2), 3.70 (3H, s, 12-CH_3), 3.61 (3H, s, 17^3-OCH_3), 3.35 (3H, s, 2-CH_3), 3.61 (3H, s, 3^4-OCH_3), 3.04 (3H, s, 7-CH_3), 2.46–2.78, 2.14–2.40 (each 2H, m, 17-CH_2CH_2), 2.34 (3H, d, *J* = 7 Hz, 3^1-CH_3), 1.81 (3H, d, *J* = 7 Hz, 18-CH_3), 1.71 (3H, t, *J* = 7.5 Hz, 8^1-CH_3), 0.28, −1.87 (each 1H, s, NH); ^{19}F NMR ($CDCl_3$) δ = −72.94. MS (FAB) found: *m*/*z* 783. calcd for $C_{44}H_{46}N_4O_6F_3$: MH^+, 783.

4.2.5. 2S-S. 1S and (*S*)-MTPA-Cl gave **2S-S** at rt = 36 min (10 mmϕ column, 3% H_2O–MeOH); vis (CH_2Cl_2) λ_{max} = 664 (rel. 0.52), 608 (0.07), 555 (0.03), 537 (0.09), 506 (0.10), 472 (0.04), 410 (1.00), 319 nm (0.20); ^{1}H NMR ($CDCl_3$) δ = 9.57 (1H, s, 10-H), 9.55 (1H, s, 5-H), 8.60 (1H, s, 20-H), 7.55 (1H, q, *J* = 7 Hz, 3-CH), 7.43 (2H, d, *J* = 8 Hz, *o*-H of Ph), 7.15 (1H, d, *J* = 7 Hz, *p*-H of Ph), 7.02 (2H, d, *J* = 8 Hz, *m*-H of Ph), 5.29 (1H, d, *J* = 20 Hz, 13^2-H_a, syn to 17-propionate), 5.14 (1H, d, *J* = 20 Hz, 13^2-H_b, anti to 17-propionate), 4.51 (1H, q, *J* = 7 Hz, 18-H), 4.33 (1H, d, *J* = 8 Hz, 17-H), 3.705 (2H, q, *J* = 8 Hz, 8-CH_2), 3.702 (3H, s, 12-CH_3), 3.61 (3H, s, 17^3-OCH_3), 3.43 (3H, s, 2-CH_3), 3.36 (3H, s, 3^4-OCH_3), 3.06 (3H, s, 7-CH_3), 2.63–2.78, 2.20–2.37 (each 2H, m, 17-CH_2CH_2), 2.26 (3H, d, *J* = 7 Hz, 3^1-CH_3), 1.81 (3H, d, *J* = 7 Hz, 18-CH_3), 1.70 (3H, t, *J* = 7.5 Hz, 8^1-CH_3), 0.27, −1.85 (each 1H, s, NH); ^{19}F NMR ($CDCl_3$) δ = −72.21. MS (FAB) found: *m*/*z* 783. calcd for $C_{44}H_{46}N_4O_6F_3$: MH^+, 783.

4.2.6. Methyl 3^1-demethyl-3^1-octadecyl-bacteriopheophorbide-*d* (4, $3^1R/3^1S$ = 1/1). A THF solution of octadecyl magnesium bromide prepared from magnesium metal turnings (0.6 g) and 1-bromooctadecane (5.8 g) in dry THF (20 mL) was added dropwise to a dry THF solution (5 mL) of aldehyde **3** (8.6 mg) with stirring at 0 °C. The reaction mixture was monitored by its visible spectra and the reaction was quenched with aqueous 1% ammonium chloride just after Q_y peak at 695 nm of the starting aldehyde disappeared, accompanied by the growth of the other Q_y peak at 660 nm of the adduct. The reaction mixture was washed with aqueous 4% sodium hydrogen carbonate and water, dried over sodium sulfate, and evaporated in vacuo. The residue

was purified with HPLC (Hitachi GL-OP100 6 mmϕ× 150 mm, MeOH, 1.5 mL/min) to give pure **4** (3^1R/3^1S = 1/1, 5.5 mg, 44% yield) at rt = 63 min; vis (CH_2Cl_2) λ_{max} = 661 (rel. 0.46), 604 (0.08), 536 (0.09), 506 (0.09), 410 nm (1.00); ^{1}H NMR ($CDCl_3$) δ = 9.65/63, 9.43, 8.50/49 (each 1H, s, 5-, 10-, 20-H), 6.17/15 (1H, t, J = 7 Hz, 3-CH), 5.22/19, 5.07/05 (each 1H, d, J = 20 Hz, 13^2-H_2), 4.45 (1H, br-q, J = 7 Hz, 18-H), 4.24 (1H, m, 17-H), 3.68 (2H, q, J = 7.5 Hz, 8-CH_2), 3.62, 3.62, 3.39/38, 3.24 (each 3H, s, 2-, 7-, 12-CH_3, 17^3-OCH_3), 2.4–2.7, 2.21–2.31 (4H + 2H, m, 3^1-CH_2, 17-CH_2CH_2), 1.78/77 (3H, d, J = 7 Hz, 18-CH_3), 1.68 (3H, t, J = 7.5 Hz, 8^1-CH_3), 1.40 (2H, m, 3^2-CH_2), 1.23, 1.18 (30H, m, 3^3-$(CH_2)_{15}$), 0.86 (3H, t, J = 7 Hz, 3^{18}-CH_3), 0.30 (1H, br, NH), −1.83/84 (1H, s, NH). MS (FAB) found: m/z 805. calcd for $C_{51}H_{73}N_4O_4$: MH^+, 805. HRMS (FAB) found: m/z 805.5631. calcd for $C_{51}H_{73}N_4O_4$: MH^+, 805.5632.

4.2.7. Zn-4R/S. According to reported procedures,[7] a 3^1-epimeric mixture of **4** was zinc-metallated and the resulting zinc complexes **Zn-4** were purified and separated by HPLC (Cosmosil 5C18-ARII 6 mmϕ×250 mm, 1% H_2O–MeOH, 1.0 mL/min) to give 3^1-epimerically pure samples **Zn-4R/S** as a dark green solid.

4.2.8. Zinc methyl 3^1-*R*-3^1-demethyl-3^1-octadecyl-bacteriopheophorbide-*d* (Zn-4R, Zn-4#1). Rt = 40 min; vis (CH_2Cl_2) λ_{max} = 648 (rel. 0.78), 600 (0.12), 553 (0.06), 512 (0.05), 422 (1.00), 402 nm (0.71); ^{1}H NMR ($CDCl_3$-8% CD_3OD) δ = 9.45, 9.29, 8.24 (each 1H, s, 5-, 10-, 20-H), 5.82 (1H, t, J = 7 Hz, 3-CH), 5.12, 4.98 (each 1H, d, J = 20 Hz, 13^2-H_2), 4.37 (1H, dq, J = 2, 7 Hz, 18-H), 4.18 (1H, br-d, J = 7 Hz, 17-H), 3.69 (2H, q, J = 7.5 Hz, 8-CH_2), 3.56, 3.44, 3.18, 3.15 (each 3H, s, 2-, 7-, 12-CH_3, 17^3-OCH_3), 2.31–2.59, 2.12–2.21 (5H + 1H, m, 3^1-CH_2, 17-CH_2CH_2), 1.75 (3H, d, J = 7 Hz, 18-CH_3), 1.66 (3H, t, J = 7.5 Hz, 8^1-CH_3), 1.29 (2H, m, 3^2-CH_2), 1.20, 1.17, 1.10 (30H, m, 3^3-$(CH_2)_{15}$), 0.81 (3H, t, J = 7 Hz, 3^{18}-CH_3). MS (FAB) found: m/z 866. calcd for $C_{51}H_{70}N_4O_4^{64}Zn$: M^+, 866.

4.2.9. Zinc methyl 3^1-*S*-3^1-demethyl-3^1-octadecyl-bacteriopheophorbide-*d* (Zn-4S, Zn-4#2). Rt = 43 min; vis (CH_2Cl_2) λ_{max} = 648 (rel. 0.78), 601 (0.12), 554 (0.06), 511 (0.05), 422 (1.00), 401 nm (0.70); ^{1}H NMR ($CDCl_3$-8% CD_3OD) δ = 9.44, 9.40, 8.23 (each 1H, s, 5-, 10-, 20-H), 5.94 (1H, t, J = 7 Hz, 3-CH), 5.11, 4.97 (each 1H, d, J = 20 Hz, 13^2-H_2), 4.35 (1H, dq, J = 2, 7 Hz, 18-H), 4.10–4.17 (1H, m, 17-H), 3.68 (2H, q, J = 7.5 Hz, 8-CH_2), 3.56, 3.46, 3.21, 3.18 (each 3H, s, 2-, 7-, 12-CH_3, 17^3-OCH_3), 2.32–2.54, 2.11–2.19 (5H + 1H, m, 3^1-CH_2, 17-CH_2CH_2), 1.72 (3H, d, J = 7 Hz, 18-CH_3), 1.64 (3H, t, J = 7.5 Hz, 8^1-CH_3), 1.31 (2H, m, 3^2-CH_2), 1.20, 1.17, 1.11 (30H, m, 3^3-$(CH_2)_{15}$), 0.81 (3H, t, J = 7 Hz, 3^{18}-CH_3). MS (FAB) found: m/z 866. calcd for $C_{51}H_{70}N_4O_4^{64}Zn$: M^+, 866.

4.2.10. MTPA ester of methyl 3^1-demethyl-3^1-octadecyl-bacteriopheophorbide-*d* (5). According to reported procedures,[7] 3^1-epimer **Zn-4R/S** was demetallated and the resulting secondary alcohol **4R/S** was esterified (see the procedures described above) to give the corresponding ester **5**.

4.2.11. 5R-R (5#1-R). **4R** and (*R*)-MTPA-Cl gave **5R-R** at rt = 76 min (6 mmϕ column, 100% MeOH); vis (CH_2Cl_2) λ_{max} = 664 (rel. 0.52), 608 (0.08), 555 (0.03), 536 (0.09), 506 (0.10), 473 (0.03), 410 (1.00), 319 nm (0.19); ^{1}H NMR ($CDCl_3$) δ = 9.57 (1H, s, 10-H), 9.54 (1H, s, 5-H), 8.60 (1H, s, 20-H), 7.37 (2H, d, J = 8 Hz, *o*-H of Ph), 7.07 (1H, t, J = 7 Hz, *p*-H of Ph), 6.90 (2H, t, J = 7.5 Hz, *m*-H of Ph), 5.30 (1H, d, J = 20 Hz, 13^2-H_a, syn to 17-propionate), 5.14 (1H, d, J = 20 Hz, 13^2-H_b, anti to 17-propionate), 4.51 (1H, q, J = 7 Hz, 18-H), 4.34 (1H, d, J = 7.5 Hz, 17-H), 3.70 (3H, s, 12-CH_3), 3.70 (2H, q, J = 7.5 Hz, 8-CH_2), 3.62 (3H, s, 17^3-OCH_3), 3.45 (3H, s, 2-CH_3), 3.29 (3H, s, 3^4-OCH_3), 3.05 (3H, s, 7-CH_3), 2.44–2.80, 2.25–2.38 (each 2H, m, 17-CH_2CH_2), 2.75, 2.49 (each 1H, m, 3^1-CH_2), 1.82 (3H, d, J = 7 Hz, 18-CH_3), 1.70 (3H, t, J = 7.5 Hz, 8^1-CH_3), 1.15–1.32 (32H, m, 3^2-$(CH_2)_{16}$), 0.86 (3H, t, J = 6 Hz, 3^{18}-CH_3), 0.29, −1.86 (each 1H, s, NH) [3-CH was hidden by $CHCl_3$ signal at 7.26 ppm]; ^{19}F NMR ($CDCl_3$) δ = −72.01. MS (FAB) found: m/z 1021. calcd for $C_{61}H_{80}N_4O_6F_3$: MH^+, 1021.

4.2.12. 5R-S (5#1-S). **4R** and (*S*)-MTPA-Cl gave **5R-S** at rt = 66 min (6 mmϕ column, 100% MeOH); vis (CH_2Cl_2) λ_{max} = 665 (rel. 0.52), 608 (0.08), 555 (0.03), 537 (0.10), 506 (0.10), 473 (0.04), 410 (1.00), 319 nm (0.20); ^{1}H NMR ($CDCl_3$) δ = 9.55 (1H, s, 10-H), 9.31 (1H, s, 5-H), 8.56 (1H, s, 20-H), 7.13 (2H, d, J = 8 Hz, *o*-H of Ph), 6.81 (1H, br-t, *p*-H of Ph), 6.64 (2H, br-t, *m*-H of Ph), 5.29 (1H, d, J = 20 Hz, 13^2-H_a, syn to 17-propionate), 5.13 (1H, d, J = 20 Hz, 13^2-H_b, anti to 17-propionate), 4.51 (1H, q, J = 7 Hz, 18-H), 4.34 (1H, d, J = 8 Hz, 17-H), 3.70 (3H, s, 12-CH_3), 3.70 (2H, J = 7.5 Hz, 8-CH_2), 3.61 (3H, s, 17^3-OCH_3), 3.60 (3H, s, 3^4-OCH_3), 3.37 (3H, s, 2-CH_3), 2.99 (3H, s, 7-CH_3), 2.51–2.89, 2.25–2.40 (each 2H, m, 17-CH_2CH_2), 2.80, 2.59 (each 1H, m, 3^1-CH_2), 1.82 (3H, d, J = 7 Hz, 18-CH_3), 1.71 (3H, t, J = 7.5 Hz, 8^1-CH_3), 1.15–1.32 (32H, m, 3^2-$(CH_2)_{16}$), 0.86 (3H, t, J = 6 Hz, 3^{18}-CH_3), 0.30, −1.82 (each 1H, s, NH) [3-CH was hidden by $CHCl_3$ signal at 7.26 ppm]; ^{19}F NMR ($CDCl_3$) δ = −72.84. MS (FAB) found: m/z 1021. calcd for $C_{61}H_{80}N_4O_6F_3$: MH^+, 1021.

4.2.13. 5S-R (5#2-R). **4S** and (*R*)-MTPA-Cl gave **5S-R** at rt = 70 min (6 mmϕ column, 100% MeOH); vis (CH_2Cl_2) λ_{max} = 664 (rel. 0.54), 608 (0.08), 555 (0.03), 536 (0.09), 506 (0.10), 473 (0.03), 410 (1.00), 319 nm (0.20); ^{1}H NMR ($CDCl_3$) δ = 9.57 (1H, s, 10-H), 9.35 (1H, s, 5-H), 8.56 (1H, s, 20-H), 7.15 (2H, d, J = 8 Hz, *o*-H of Ph), 6.85 (1H, br-t, *p*-H of Ph), 6.69 (2H, t, J = 8 Hz, *m*-H of Ph), 5.31 (1H, d, J = 20 Hz, 13^2-H_a, syn to 17-propionate), 5.15 (1H, d, J = 20 Hz, 13^2-H_b, anti to 17-propionate), 4.52 (1H, q, J = 7 Hz, 18-H), 4.34 (1H, d, J = 8 Hz, 17-H), 3.71 (3H, s, 12-CH_3), 3.69 (2H, J = 7.5 Hz, 8-CH_2), 3.60 (3H, s, 17^3-OCH_3), 3.50 (3H, s, 3^4-OCH_3), 3.34 (3H, s, 2-CH_3), 3.04 (3H, s, 7-CH_3), 2.57–2.82, 2.28–2.33 (each 2H, m, 17-CH_2CH_2), 2.80, 2.71 (each 1H, m, 3^1-CH_2), 1.84 (3H, d, J = 7 Hz, 18-CH_3), 1.72 (3H, t, J = 7.5 Hz, 8^1-CH_3), 1.24–1.29 (32H, m, 3^2-$(CH_2)_{16}$), 0.87 (3H, t, J = 6 Hz, 3^{18}-CH_3), 0.30, −1.87 (each 1H, s, NH) [3-CH was hidden by $CHCl_3$ signal at 7.26 ppm]; ^{19}F NMR ($CDCl_3$) δ = −72.81. MS (FAB) found: m/z 1021. calcd for $C_{61}H_{80}N_4O_6F_3$: MH^+, 1021.

4.2.14. 5S-S (5#2-S). 4S and (*S*)-MTPA-Cl gave 5S-S at rt = 80 min (6 mmϕ column, 100% MeOH); vis (CH_2Cl_2) λ_{max} = 664 (rel. 0.52), 608 (0.07), 555 (0.03), 536 (0.09), 506 (0.10), 472 (0.04), 410 (1.00), 319 nm (0.19); ^{1}H NMR ($CDCl_3$) δ = 9.58 (1H, s, 10-H), 9.56 (1H, s, 5-H), 8.61 (1H, s, 20-H), 7.39 (2H, d, *J* = 8 Hz, *o*-H of Ph), 7.10 (1H, t, *J* = 7 Hz, *p*-H of Ph), 6.94 (2H, t, *J* = 8 Hz, *m*-H of Ph), 5.31 (1H, d, *J* = 20 Hz, 13^2-H_a, syn to 17-propionate), 5.15 (1H, d, *J* = 20 Hz, 13^2-H_b, anti to 17-propionate), 4.51 (1H, q, *J* = 7 Hz, 18-H), 4.34 (1H, d, *J* = 8 Hz, 17-H), 3.72 (3H, s, 12-CH_3), 3.72 (2H, *J* = 7.5 Hz, 8-CH_2), 3.62 (3H, s, 17^3-OCH_3), 3.45 (3H, s, 2-CH_3), 3.30 (3H, s, 3^4-OCH_3), 3.08 (3H, s, 7-CH_3), 2.45–2.79, 2.21–2.36 (each 2H, m, 17-CH_2CH_2), 2.74, 2.63 (each 1H, m, 3^1-CH_2), 1.84 (3H, d, *J* = 7 Hz, 18-CH_3), 1.71 (3H, t, *J* = 7.5 Hz, 8^1-CH_3), 1.24–1.29 (32H, m, 3^2-$(CH_2)_{16}$), 0.87 (3H, t, *J* = 6 Hz, 3^{18}-CH_3), 0.29, −1.84 (each 1H, s, NH) [3-CH was hidden by $CHCl_3$ signal at 7.26 ppm]; ^{19}F NMR ($CDCl_3$) δ = −72.02. MS (FAB) found: *m*/*z* 1021. calcd for $C_{61}H_{80}N_4O_6F_3$: MH^+, 1021.

4.2.15. Conversion of MTPA ester to secondary alcohol. Methanolysis of MTPA ester was done according to a slightly modified version of the procedure reported by Tamiaki et al.[14] Anhydrous potassium carbonate (10 mg) was added to a methanol solution (200 μL) of MTPA ester **2**/**5** (ca. 2 μmol) and the solution was stirred for 2 h at 0 °C. The reaction mixture was diluted with dichloromethane (20 mL), washed with water, dried over sodium sulfate, and evaporated at a reduced pressure. The residue was dissolved in methanol and purified with HPLC (Cosmosil 5C18-ARII 6 mmϕ×250 mm, MeOH, 1.5 mL/min) to give the corresponding alcohol **1**/**4** as a pure form.

Acknowledgements

This work was partially supported by Grants-in-Aid for Scientific Research (No. 15033271) on Priority Areas (417) from the Ministry of Education, Culture, Sports, Science and Technology (MEXT) of the Japanese Government and for Scientific Research (B) (No. 15350107) from Japan Society for the Promotion of Science (JSPS).

References and notes

1. Carr, H. S.; Winge, D. R. *Acc. Chem. Res.* **2003**, *36*, 309.
2. Mizoguchi, T.; Oh-oka, H.; Tamiaki, H. *Program and Abstracts*, 11th International Symposium on Phototrophic Prokaryotes, Tokyo, Aug. 24–29, 2003, P031.
3. Smith, K. M. In *The Porphyrin Handbook, Vol. 13, Chapter 81*; Kadish, K., Smith, K. M., Guilard, R., Eds.; Academic Press: San Diego, 2003; pp 157–182.
4. Tamiaki, H.; Omoda, M.; Saga, Y.; Morishita, H. *Tetrahedron* **2003**, *59*, 4337.
5. Risch, N.; Brockmann, H., Jr. *Liebigs Ann. Chem.* **1976**, 578.
6. Brockmann, H., Jr.; Tacke-Karimdadian, R. *Liebigs Ann. Chem.* **1979**, 419.
7. Tamiaki, H.; Takeuchi, S.; Tsudzuki, S.; Miyatake, T.; Tanikaga, R. *Tetrahedron* **1998**, *54*, 6699.
8. Miyatake, T.; Oba, T.; Tamiaki, H. *ChemBioChem.* **2001**, *2*, 335. Mizoguchi, T.; Saga, Y.; Tamiaki, H. *Photochem. Photobiol. Sci.* **2002**, *1*, 780. Saga, Y.; Matsuura, K.; Tamiaki, H. *Photochem. Photobiol.* **2001**, *74*, 72. Kunieda, M.; Mizoguchi, T.; Tamiaki, H. *Photochem. Photobiol.* **2004**, *79*, 55.
9. Sullivan, G. R.; Dale, J. A.; Mosher, H. S. *J. Org. Chem.* **1973**, *38*, 2143.
10. Ohtani, I.; Kusumi, T.; Kashman, Y.; Kakisawa, H. *J. Am. Chem. Soc.* **1991**, *113*, 4092.
11. Kelly, D. R. *Tetrahedron: Asym.* **1999**, *10*, 2927.
12. Smith, K. M.; Bisset, G. M. F.; Bushell, M. *J. Org. Chem.* **1980**, *45*, 2218.
13. Tamiaki, H.; Takeuchi, S.; Tanikaga, R.; Balaban, S. T.; Holzwarth, A. R.; Schaffner, K. *Chem. Lett.* **1994**, 401.
14. Tamiaki, H.; Kouraba, M.; Takeda, K.; Kondo, S.; Tanikaga, R. *Tetrahedron: Asym.* **1998**, *9*, 2101.
15. Tamiaki, H.; Shimono, Y.; Rattray, A. G. M.; Tanikaga, R. *Bioorg. Med. Chem. Lett.* **1996**, *6*, 2085.
16. Tamiaki, H.; Tomida, T.; Miyatake, T. *Bioorg. Med. Chem. Lett.* **1997**, *7*, 1415.
17. Balaban, T. S.; Tamiaki, H.; Holzwarth, A. R.; Schaffner, K. J. *Phys. Chem. B* **1997**, *101*, 3424.
18. Yagai, S.; Miyatake, T.; Shimono, Y.; Tamiaki, H. *Photochem. Photobiol.* **2001**, *73*, 153.
19. Chiefari, J.; Griebenow, K.; Griebenow, N.; Balaban, T. S.; Holzwarth, A. R.; Schaffner, K. *J. Phys. Chem.* **1995**, *99*, 1357.
20. Tamiaki, H.; Kitamoto, H.; Nishikawa, A.; Hibino, T.; Shibata, R. In *Biomolecular Chemistry — A Bridge for the Future*, Scientific Program Committee of ISBC 2003, Ed.; Maruzen: Tokyo, 2003, pp 184–187.
21. Umetsu, M.; Seki, R.; Kadota, T.; Wang, Z.-Y.; Adschiri, T.; Nozawa, T. *J. Phys. Chem. B* **2003**, *107*, 9876.
22. Yagai, S.; Miyatake, T.; Tamiaki, H. *J. Org. Chem.* **2002**, *67*, 49.
23. Tamiaki, H.; Holzwarth, A. R.; Schaffner, K. *Photosynth. Res.* **1994**, *41*, 245.
24. Tamiaki, H. *Coord. Chem. Rev.* **1996**, *148*, 183. Blankenship, R. E.; Matsuura, K. In *Light-Harvesting Antennas in Photosynthesis*, Chapter 6; Green, B. R.; Parson, W. W. Eds.; Kluwer: Dordrecht, 2003; pp 195–217.
25. Tamiaki, H.; Amakawa, M.; Shimono, Y.; Tanikaga, R.; Holzwarth, A. R.; Schaffner, K. *Photochem. Photobiol.* **1996**, *63*, 92. Tamiaki, H.; Miyata, S.; Kureishi, Y.; Tanikaga, R. *Tetrahedron* **1996**, *52*, 12421.